# [Bi$_6$Mo$_3$(CO)$_9$]$^{4-}$: A multiple σ-aromatic cluster containing distorted Bi$_6$ triangular prism

Lei Qiao, Dandan Chen, Jun Zhu, Alvaro Munñz-Castro, Zhong-Ming Sun*

## Content

## 1. Experimental Procedures

All manipulations and reactions were performed under a nitrogen atmosphere using standard Schlenk or glovebox techniques. En (Aldrich, 99%) and tol (Aldrich, 99.8%) were freshly distilled by sodium/benzophenone under $N_2$ atmosphere, and stored in $N_2$ prior to use. 2.2.2-crypt (4,7,13,16,21,24-Hexaoxa-1,10-diazabicyclo (8.8.8) hexacosane, purchased from Sigma-Aldirich, 98%) was dried in vacuum for one day prior to use. $K_5Bi_4$ was synthesized by heating a stoichiometric mixture of the elements at 600 °C for two days in a niobium tube. $(MeCN)_3Mo(CO)_3$ was prepared according to literature methodology.[1]

**Synthesis of [K(2.2.2-crypt)]$_4$[Bi$_6$Mo$_3$(CO)$_9$] (1):**

In a 10 mL vial, $K_5Bi_4$ (50 mg, 0.05 mmol) and 2.2.2-crypt (80 mg, 0.21 mmol) were dissolved in en (2 mL). In a second vial, 30 mg (0.10 mmol) $(MeCN)_3Mo(CO)_3$ was dissolved in 1 mL acetonitrile. The yellow acetonitrile solution was dropwise added to en solution while stirring vigorously. The resulting red brown solution was then stirred 0.5h, then heated at 95 °C for 1h and at 70 °C for another 1h. The reaction mixture was subsequently centrifuged (5000 rmp) and filtered through glass wool and transferred to a test tube, and then carefully layered with toluene (3 mL). After 5 days, dark block crystals of [K(2.2.2-crypt)]$_4$[Bi$_6$Mo$_3$(CO)$_9$] were obtained at the yield of 35% based on the precursor $K_5Bi_4$.

**Synthesis of [K(2.2.2-crypt)]$_3$[Bi$_3$Mo$_2$(CO)$_6$] (2):**

[K(2.2.2-crypt)]$_3$[Bi$_3$Mo$_2$(CO)$_6$] was isolated in a similar way to the synthesis of compound **1**, except that smaller dosage of $(MeCN)_3Mo(CO)_3$ (15 mg, 0.05 mmol) was used to react with the precursor $K_5Bi_4$. Metallic grayish black crystals of [K(2.2.2-crypt)]$_3$[Bi$_3$Mo$_2$(CO)$_6$] were obtained at the yield of 40% based on the precursor $K_5Bi_4$.

**X-ray Diffraction:**

Suitable single crystals were selected for X-ray diffraction analyses. Crystallographic data were collected on Rigaku XtalAB Pro MM007 DW diffractometer with graphite monochromated Cu Kα radiation (λ = 1.54184 Å). Structures were solved using direct methods and then refined using SHELXL-2014 and Olex2[2-4] to convergence, in which all the non-hydrogen atoms were refined anisotropically during the final cycles. All hydrogen atoms of the organic molecule were placed by geometrical considerations and were added to the structure factor calculation. A summary of the crystallographic data for the title compound was listed in Table **S1**, and selected bond distances were given in Table **S2**. CCDC entries 2055162 and 2055164 for compound **1** and **2** contain the supplementary crystallographic data for this paper. These data can be obtained free of charge from the Cambridge Crystallographic Data Centre (www.ccdc.cam.ac.uk/data_request/cif).

**Electrospray Ionization Mass Spectrometry (ESI-MS) Investigations:**

Negative ion mode ESI-MS of the acetonitrile solutions of the single crystal of [K(2.2.2-crypt)]$_4$[Bi$_6$Mo$_3$(CO)$_3$] were measured on an LTQ linear ion trap spectrometer by Agilent Technologies ESI-TOF-MS (6230). The spray voltage was 5.48 kV and the capillary temperature was kept at 300 °C. The capillary voltage was 30 V. The samples were made up inside a glovebox under a nitrogen atmosphere and rapidly transferred to the spectrometer in an airtight syringe by direct infusion with a Harvard syringe pump at 0.2 mL/ min.

**Energy Dispersive X-ray (EDX) Spectroscopic Analysis:**

EDX analysis on the title compound was performed using a scanning electron microscope (FE-SEM, JEOL JSM-7800F, Japan). Data acquisition was performed with an acceleration voltage of 15 kV and an accumulation time of 60 s.

**Quantum chemical methods:**

Geometry optimizations and induced magnetic fields were computed with the Amsterdam Density Functional (ADF) package of program, version 2019.103[5]. A triple-zeta quality basis set of Slater-type orbitals supplemented by a single set of polarization functions (TZP) was used for all geometry optimizations, adopting the PBE0 functional [6]. The confining effect of cations in the solid state were

simulated by using a continuum solvent model (COSMO) with a dielectric constant of $\varepsilon_r$=78.39. Adaptive natural density partitioning (AdNDP) analysis[7] was carried out at the PBE0/def2-TZVP//PBE0/TZP level of theory, using the Gaussian 09[8] and the Multiwfn 3.7 softwares[9]. For EDDB (CAM-B3LYP/def2-TZVP//PBE0/TZP) and PIO (PBE0/def2-TZVP//PBE0/TZP) calculations, the density matrices of natural atomic orbitals (DMNAO) were obtained using the Gaussian 16 software package[10], which were further analyzed by the *RunEDDB* and *PIO* codes available at *http://eddb.pl/runeddb/* and *https://github.com/jxzhangcc/PIO*, respectively. MCI calculations in the NAO basis were conducted using the Multiwfn software. Calculations for the magnetic criteria of aromaticity were carried out by using the ADF program at the GIAO formalism within the relativistic ZORA-OPBE/TZ2P level[11,12] of theory, which allows to determine both shielding and deshielding surfaces for averaged and specific orientations of the applied field ($B^{ind}_i$; i=x, y, z), and NICS values at certain points within the characterized cluster.

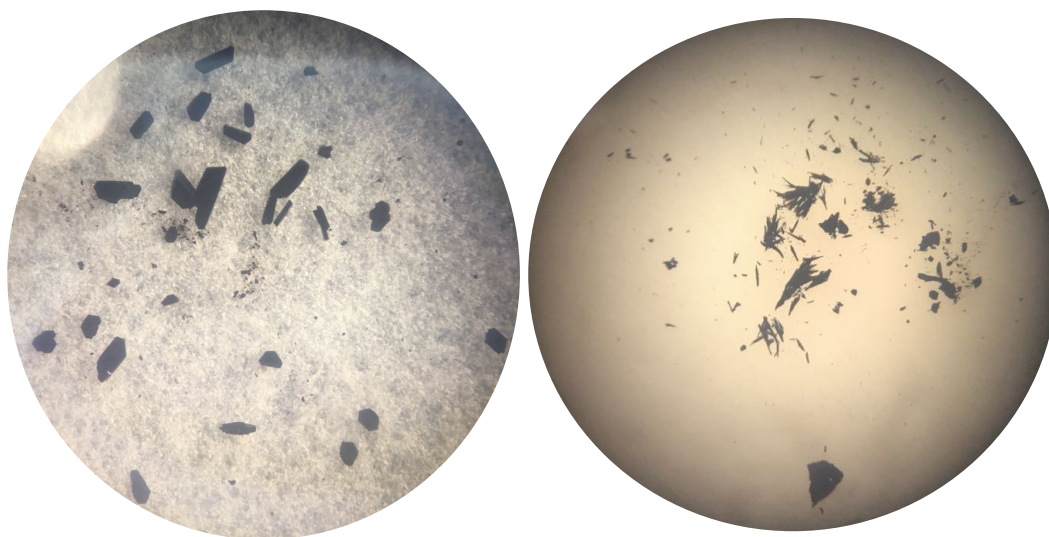## 2. Crystallographic Supplementary Information



**Figure S1.** Crystals of [K(2.2.2-crypt)]$_4$[Bi$_6$Mo$_3$(CO)$_9$] (left) and [K(2.2.2-crypt)]$_3$[Bi$_3$Mo$_2$(CO)$_6$] (right) dispersed silicon oil.

**Table S1.** X-ray measurements and structure solutions of [K(2.2.2-crypt)]$_4$[Bi$_6$Mo$_3$(CO)$_3$] and [K(2.2.2-crypt)]$_3$[Bi$_3$Mo$_2$(CO)$_3$].
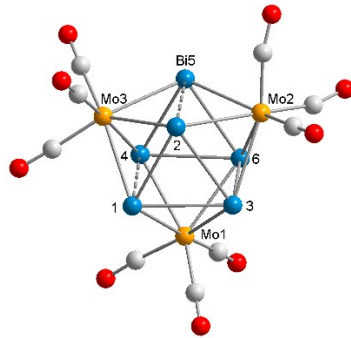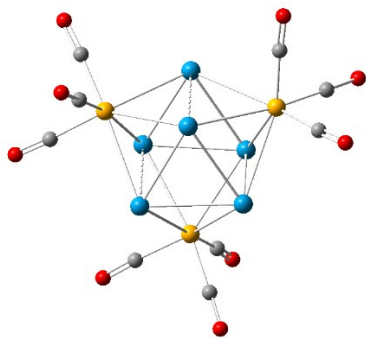
| Compound | 1 | 2 |
|---|---|---|
| Empirical formula | C$_{81}$H$_{144}$Bi$_6$K$_4$Mo$_3$N$_8$O$_{33}$ | C$_{120}$H$_{216}$Bi$_6$K$_6$ Mo$_4$N$_{12}$O$_{48}$ |
| Formula weight | 3456.14 | 4467.28 |
| Crystal system | triclinic | monoclinic |
| Space group | *P*-1 | *P*2$_1$/c |
| a /Å | 15.0576(2) | 20.4639(10) |
| b /Å | 16.1907(3) | 14.4411(10) |
| *c* /Å | 30.1290(3) | 27.5222(2) |
| *α*/° | 76.0792(11) | 90 |
| *β*/° | 77.6588(10) | 105.1840 |
| *γ*/° | 62.9932(15) | 90 |
| *V* /Å$^3$ | 6305.52(17) | 7849.45(9) |

| Z | 2 | 2 |
|---|---|---|
| $\rho_{calc}$ /g·cm$^{-3}$ | 1.820 | 1.890 |
| $\mu(Cu_{K\alpha})$ /mm$^{-1}$ | 20.172 | 17.535 |
| F(000) | 3300.0 | 4368.0 |
| $2\Theta$ range /° | 7.952 to 133.996 | 8.742 to 152.824 |
| Reflections collected / unique | 61639/22367 | 33908/15571 |
| Data / restraints / parameters | 22367/7370/1327 | 15571/0/883 |
| $R_1/wR_2$ ($I>2\sigma(I)$)$^a$ | 0.0927, 0.2488 | 0.0321, 0.0838 |
| $R_1/wR_2$ (all data) | 0.0996, 0.2556 | 0.0363, 0.0860 |
| GooF (all data)$^b$ | 1.027 | 1.056 |
| Data completeness | 99.6 | 98.9 |
| Max. peak/hole /e$^-$·Å$^{-3}$ | 7.00/-5.14 | 1.29/-1.83 |

$^a$ $R_1= \sum||F_o|-|F_c||/\sum|F_o|$; $wR_2 = \{\sum w[(F_o)^2-(F_c)^2]^2/\sum w[(F_o)^2]^2\}^{1/2}$

$^b$ $GooF = \{\sum w[(Fo)^2-(Fc)^2]^2/(n-p)\}^{1/2}$

**Table S2.** Selected bond lengths (in Å) of the experiment and optimized geometries of $[Bi_6Mo_3(CO)_3]^{4-}$ at the PBE0/TZP level of theory.

| | Experimental | Calculation |
|---|---|---|
| |  |  |
| Bi1-Bi2 | 3.0664(9) | 3.09723 |
| Bi2-Bi3 | 3.1989(12) | 3.18552 |
| Bi1-Bi3 | 3.1164(9) | 3.11645 |
| Bi3-Bi6 | 3.1740(7) | 3.18963 |
| Bi4-Bi5 | 3.1027(9) | 3.08804 |
| Bi5-Bi6 | 3.1555(12) | 3.19497 |
| Bi4-Bi6 | 3.1463(9) | 3.11394 |
| Mo1-Bi1 | 3.0111(13) | 3.08468 |
| Mo1-Bi3 | 3.0348(10) | 3.05670 |
| Mo1-Bi4 | 2.9947(17) | 3.09851 |
| Mo1-Bi6 | 2.9847(12) | 3.05508 |
| Mo2-Bi2 | 3.0050(14) | 3.09583 |
| Mo2-Bi3 | 2.9948(16) | 3.08440 |
| Mo2-Bi5 | 3.0066(16) | 3.09652 |
| Mo2-Bi6 | 2.9986(14) | 3.07493 |
| Mo3-Bi1 | 2.9961(17) | 3.08210 |
| Mo3-Bi2 | 2.9893(14) | 3.05581 |
| Mo3-Bi4 | 2.9943(15) | 3.08694 |

| Mo3-Bi5 | 2.9754(12) | 3.05775 |

The [K(2,2,2-crypt)]⁺ cations and oxygen atoms in the anionic cluster (compound **1**) appear to disorder problem, which is solved by the "mSplit" process in Olex 2.1.3. The specific bond angles and distances were constrained by "Dfix" order. The invalid reflections of compound were omitted without affecting the accuracy of the results. Residual density is mainly due to the absorption of those heavy atoms (Bi).
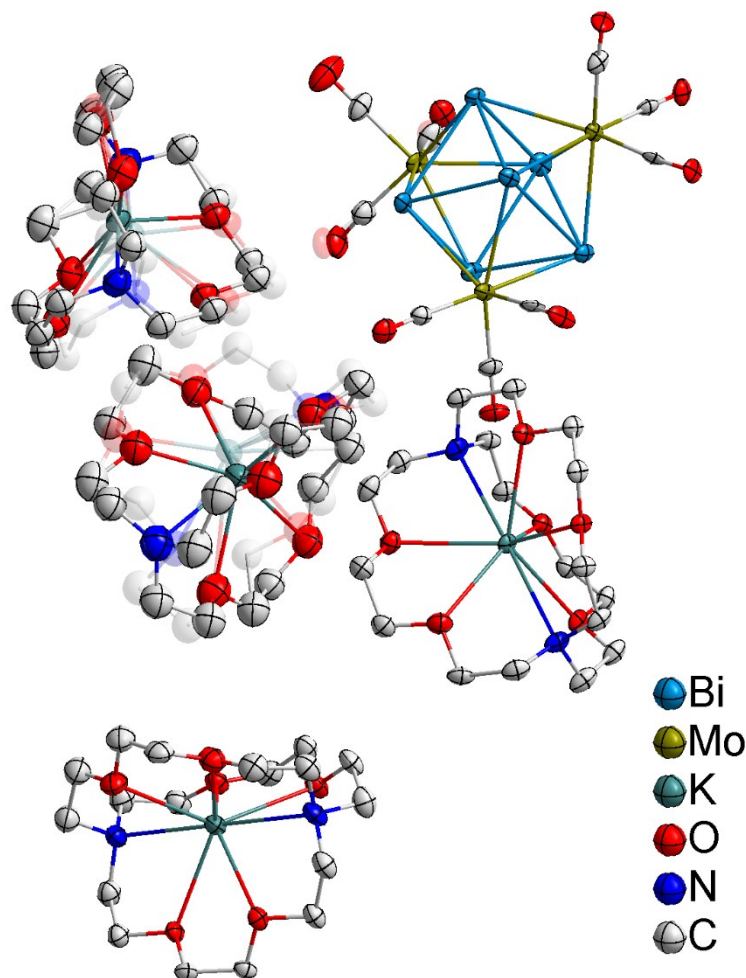


**Figure S2.** Asymmetric unit of [K(2.2.2-crypt)]$_4$[Bi$_6$Mo$_3$(CO)$_3$]. Thermal ellipsoids are drawn at 50% probability. The H atoms are omitted for clarity. The disordered fragments in the two 2.2.2-crypt molecules and the disordered oxygen atoms in the anionic cluster are shown at 70% transparency.
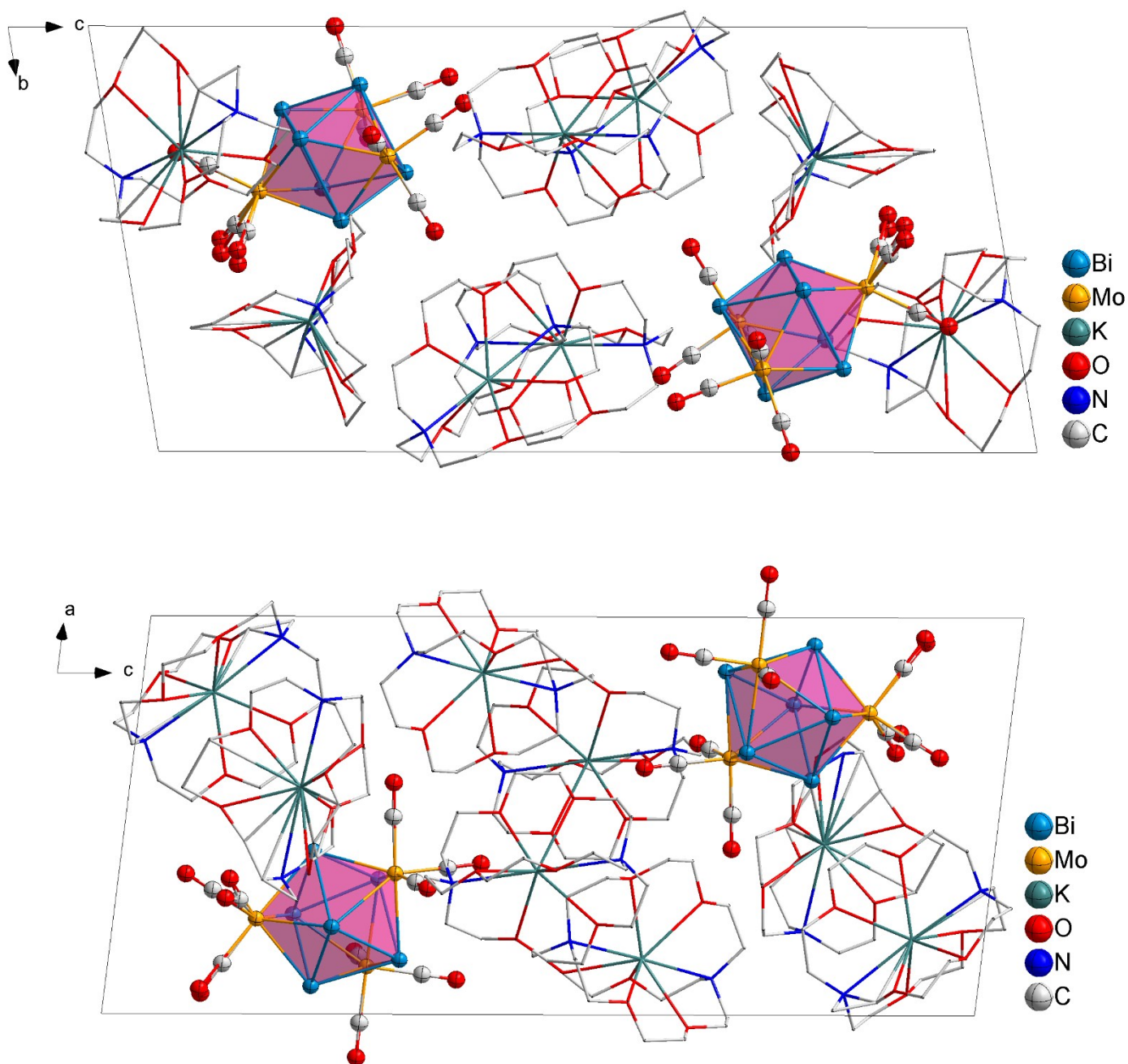
**Figure S3.** Different directions of unit cell of compound **1**. Minor component in the cluster site are omitted for clarity.

## 3. ESI-MS Studies

The ESI-MS of the acetonitrile solution of the crystals of [K(2.2.2-crypt)]$_4$[Bi$_6$Mo$_3$(CO)$_9$]·(**Figure S4**) indicated that a series of Bi-Mo binary clusters (including Bi$_4$Mo$_3$, Bi$_5$Mo$_3$, Bi$_6$Mo$_3$ and Bi$_7$Mo$_3$) with a different number of ligands are stable in solution. Measured and simulated isotope distributions for all species were shown in the **Figures S5-16**.
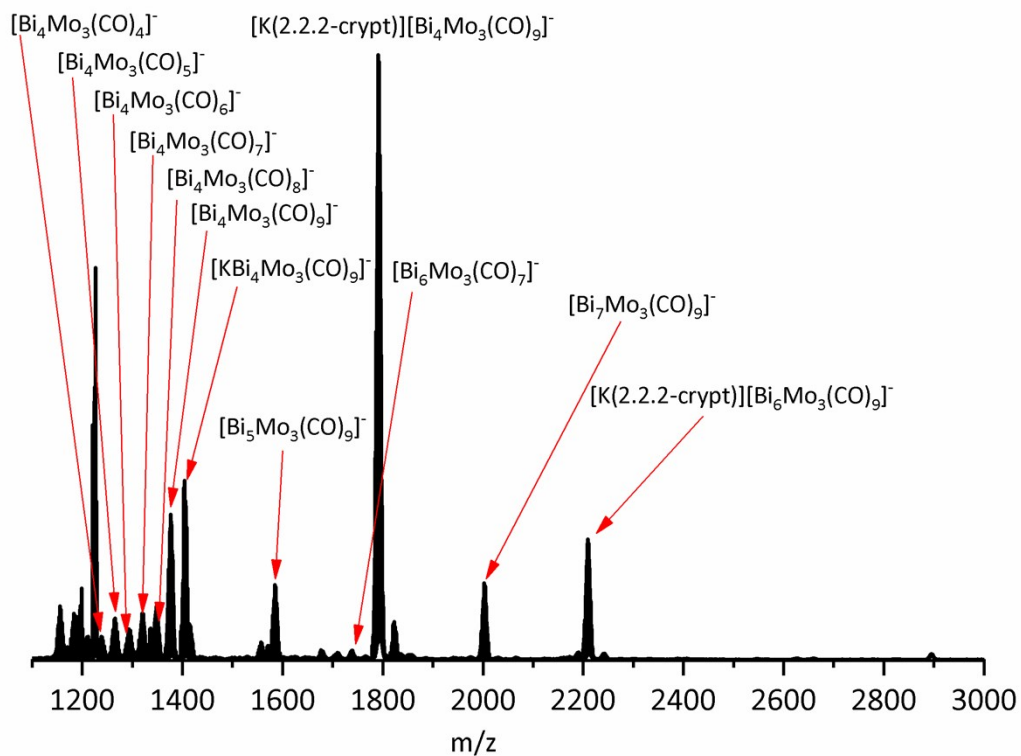
**Figure S4**. Overview ESI mass spectrum in negative ion mode of a freshly dissolved crystalline sample of $[K(2.2.2\text{-crypt})]_4[Bi_6Mo_3(CO)_9]$ in acetonitrile.
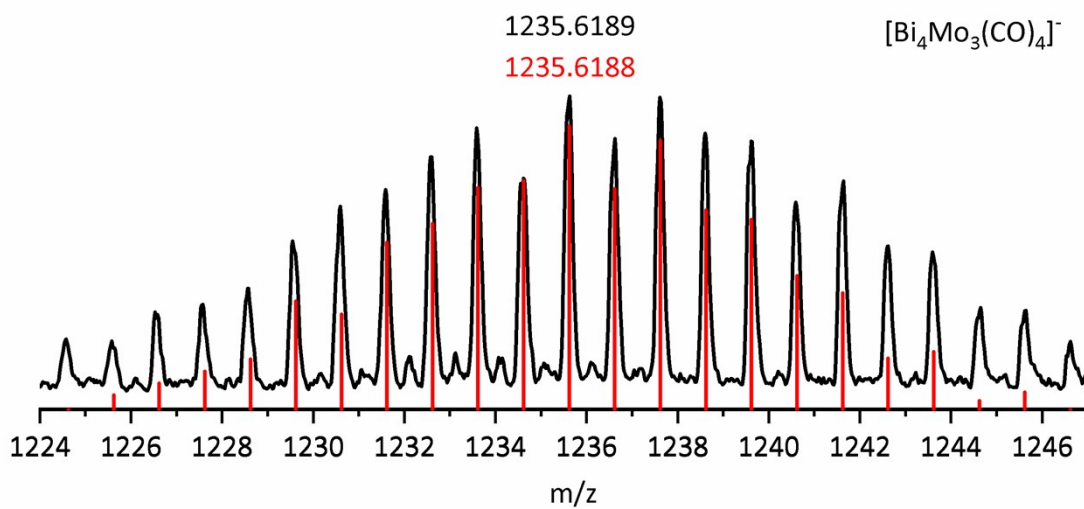


**Figure S5.** Measured (black) and simulated (red) spectrum of the fragment $[Bi_4Mo_3(CO)_4]^-$.

1263.6104
1263.6137
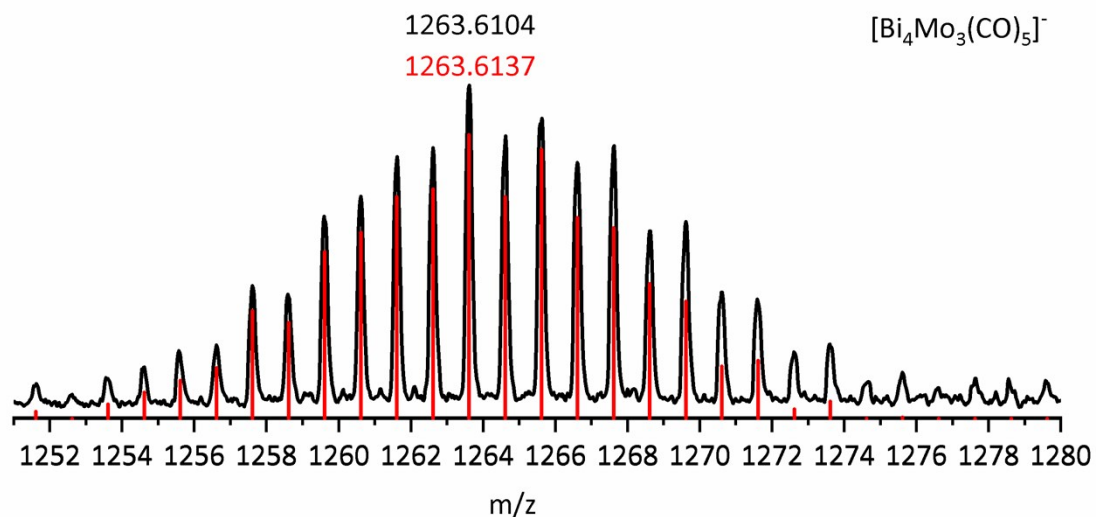$[Bi_4Mo_3(CO)_5]^-$

m/z

**Figure S6.** Measured (black) and simulated (red) spectrum of the fragment $[Bi_4Mo_3(CO)_5]^-$.

1291.6090
1291.6087
$[Bi_4Mo_3(CO)_6]^-$

m/z
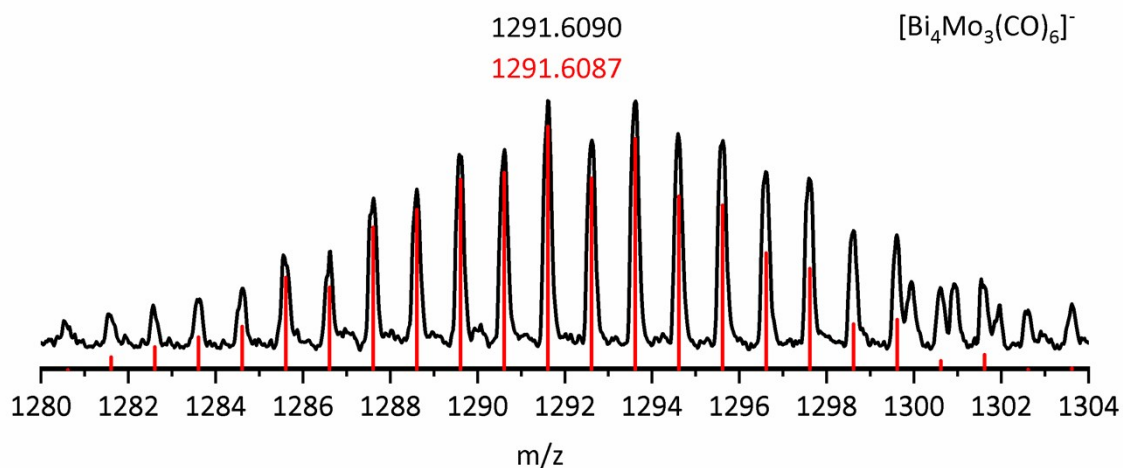
**Figure S7.** Measured (black) and simulated (red) spectrum of the fragment $[Bi_4Mo_3(CO)_6]^-$.

1319.6050
1319.6036
$[Bi_4Mo_3(CO)_7]^-$

m/z
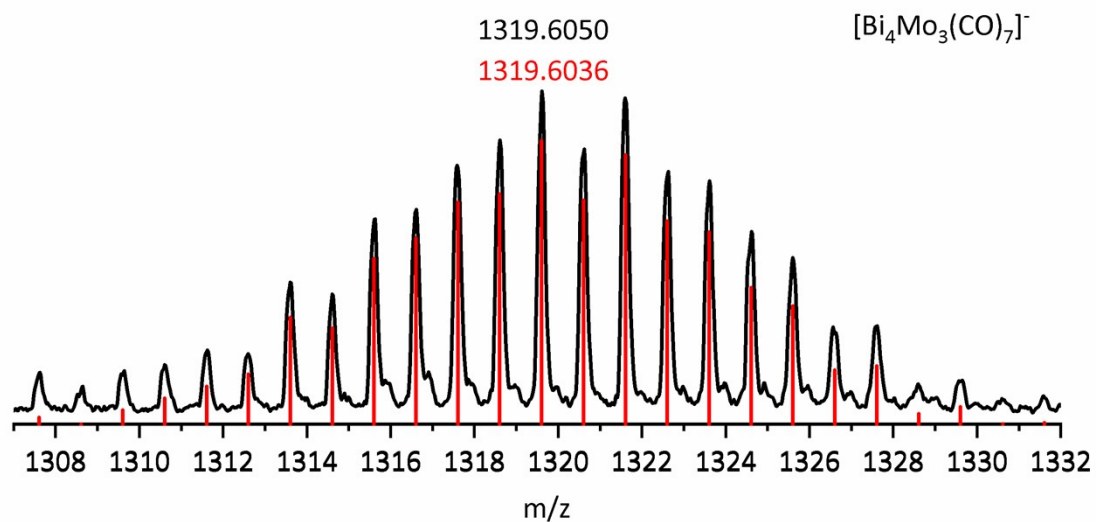
**Figure S8.** Measured (black) and simulated (red) spectrum of the fragment $[Bi_4Mo_3(CO)_7]^-$.

1347.5942
1347.5986
$[Bi_4Mo_3(CO)_8]^-$

1336 1338 1340 1342 1344 1346 1348 1350 1352 1354 1356 1358 1360
m/z
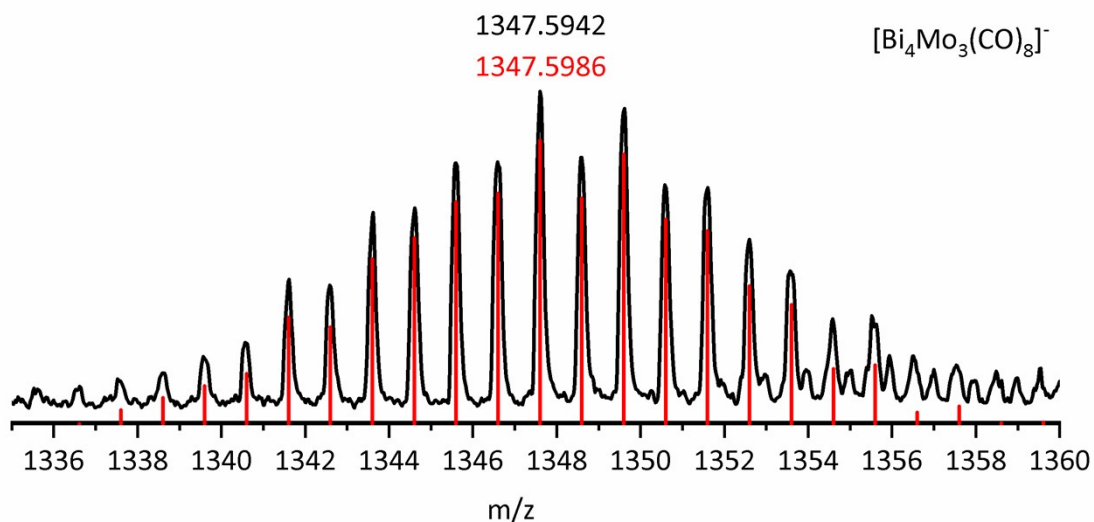
**Figure S9.** Measured (black) and simulated (red) spectrum of the fragment $[Bi_4Mo_3(CO)_8]^-$.

1375.6018
1375.5936
$[Bi_4Mo_3(CO)_9]^-$

1364 1366 1368 1370 1372 1374 1376 1378 1380 1382 1384 1386 1388
m/z
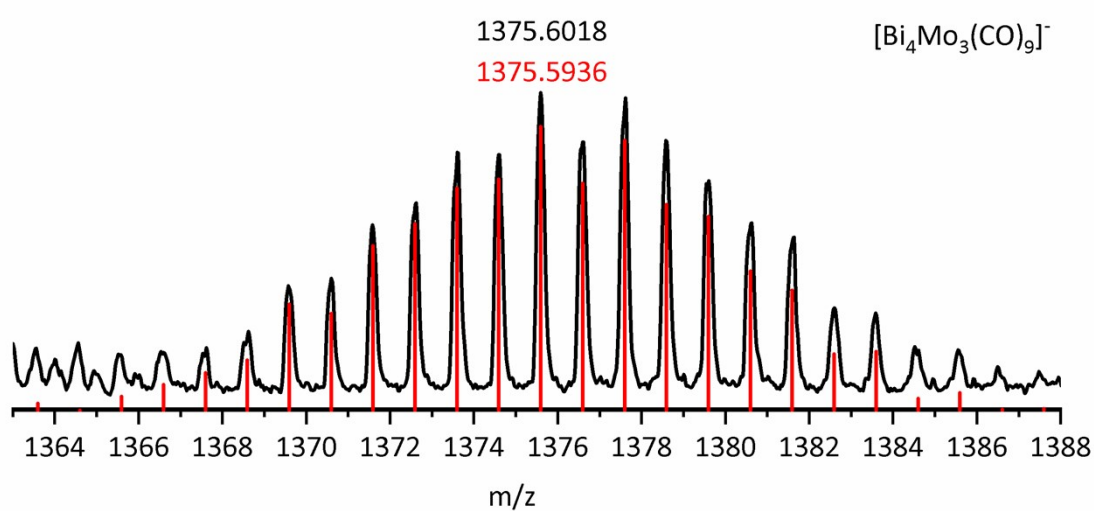
**Figure S10.** Measured (black) and simulated (red) spectrum of the fragment $[Bi_4Mo_3(CO)_9]^-$.

1414.5604
1414.5572
$[KBi_4Mo_3(CO)_9]^-$

1402 1404 1406 1408 1410 1412 1414 1416 1418 1420 1422 1424 1426
m/z
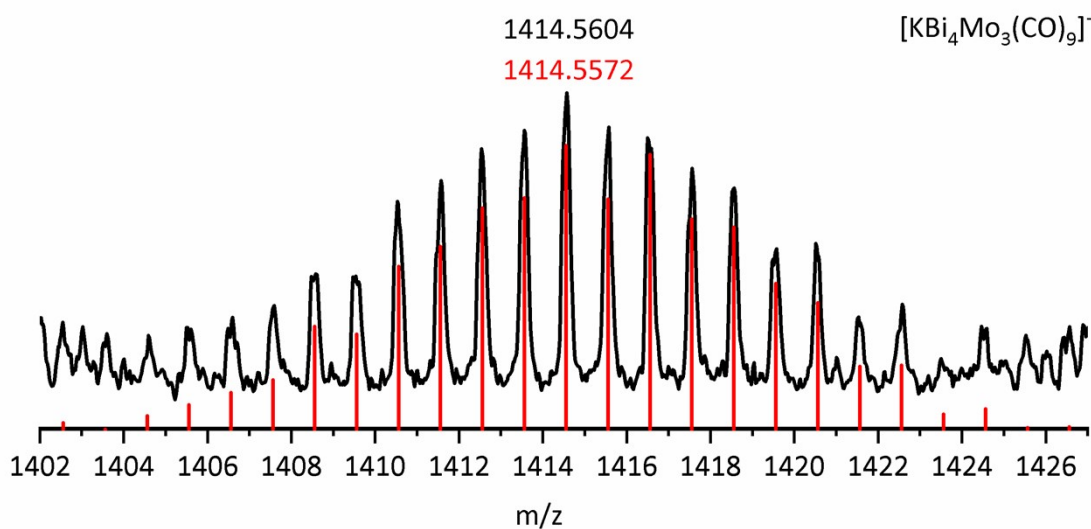
**Figure S11.** Measured (black) and simulated (red) spectrum of the fragment $[KBi_4Mo_3(CO)_9]^-$.

1790.8135     {[K(2.2.2-crypt)][Bi$_4$Mo$_3$(CO)$_9$]}$^-$
1790.8151

**Figure S12.** Measured (black) and simulated (red) spectrum of the fragment {[K(2.2.2-ccrypt)][Bi$_4$Mo$_3$(CO)$_9$]}$^-$.

1584.5699     [Bi$_5$Mo$_3$(CO)$_9$]$^-$
1584.5739

**Figure S13.** Measured (black) and simulated (red) spectrum of the fragment [Bi$_5$Mo$_3$(CO)$_9$]$^-$.

1737.5511     [Bi$_6$Mo$_3$(CO)$_7$]$^-$
1737.5644

**Figure S14.** Measured (black) and simulated (red) spectrum of the fragment [Bi$_6$Mo$_3$(CO)$_7$]$^-$.
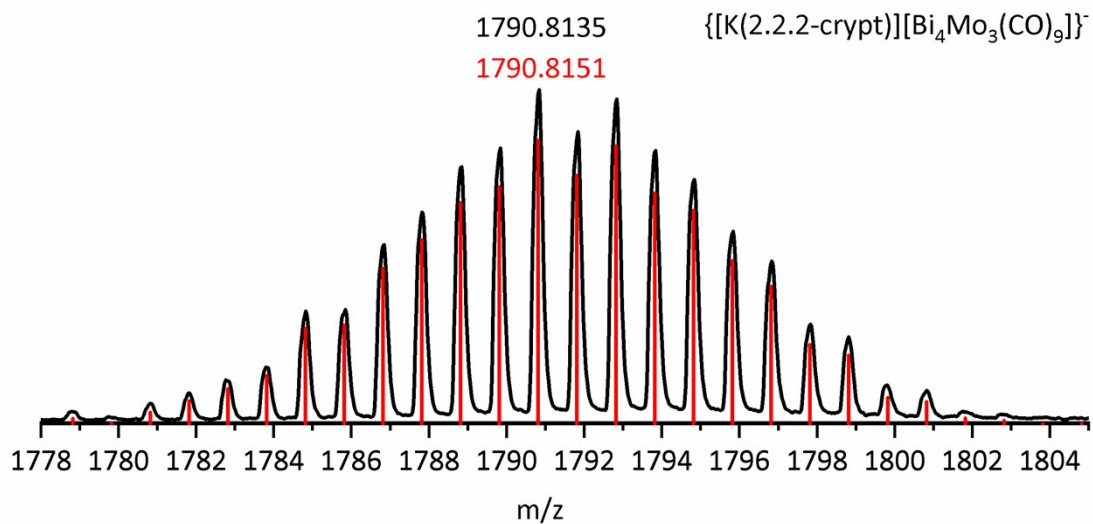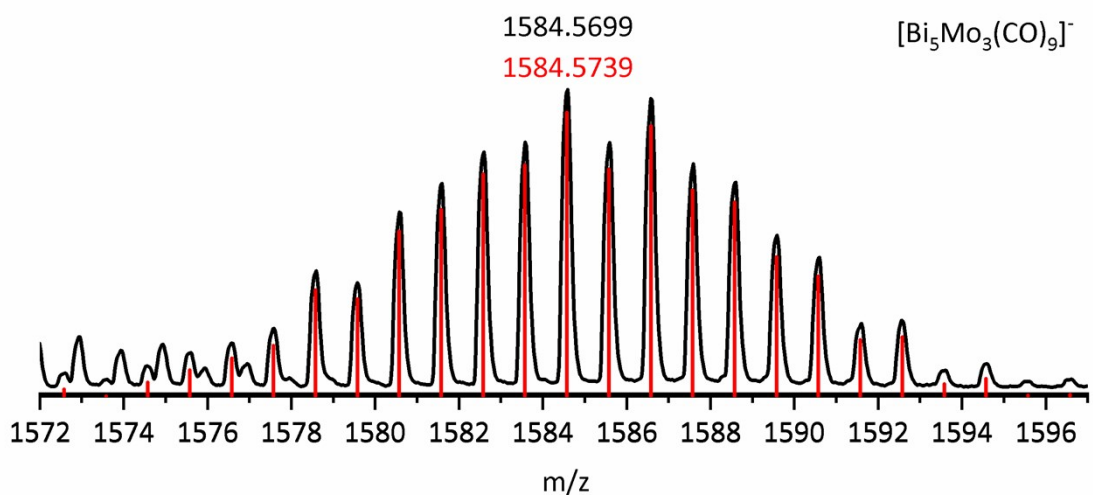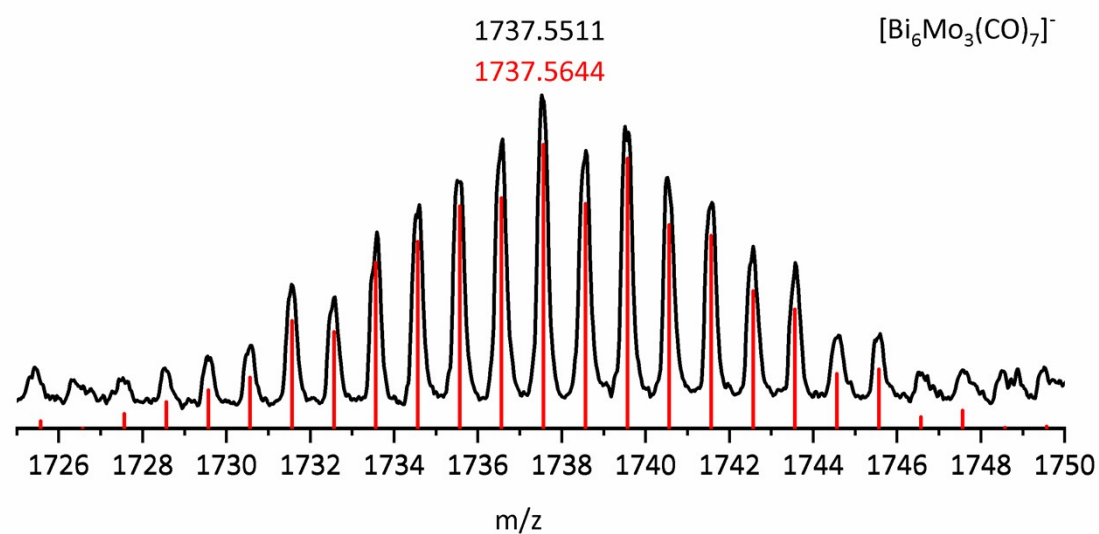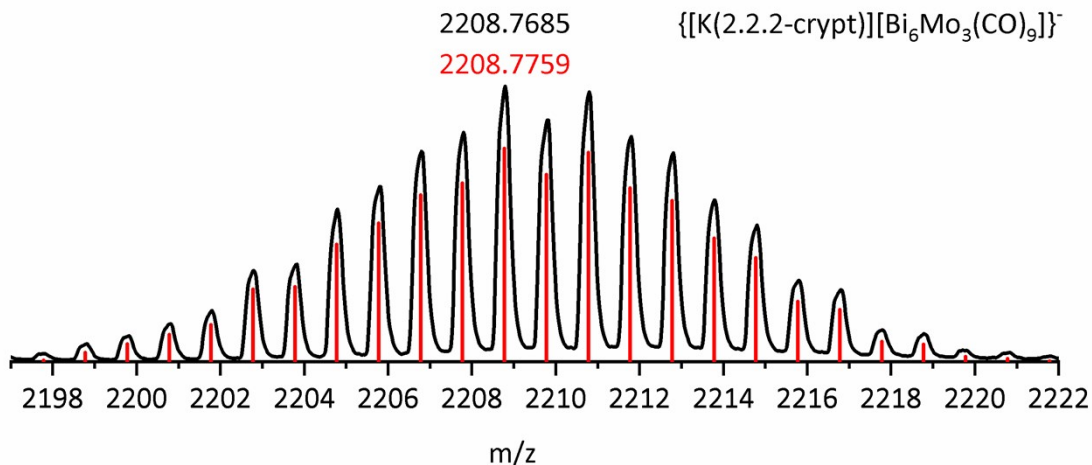
**Figure S15.** Measured (black) and simulated (red) spectrum of the fragment {[K(2.2.2-crypt)][Bi$_6$Mo$_3$(CO)$_9$]}$^-$.
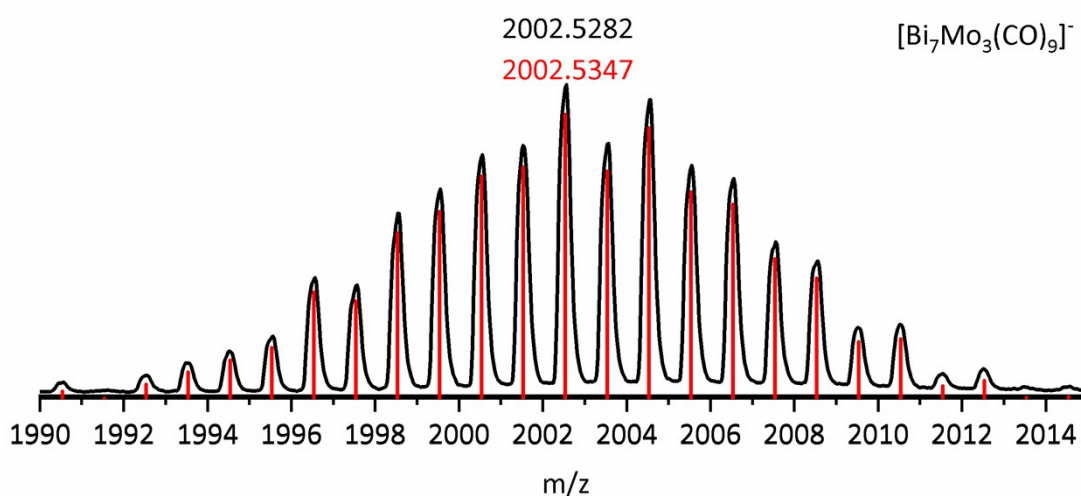


**Figure S16.** Measured (black) and simulated (red) spectrum of the fragment [Bi$_7$Mo$_3$(CO)$_9$]$^-$.

## 4. Energy Dispersive X-ray (EDX) Spectroscopic Analysis

The results of EDX analysis on [K(2.2.2-crypt)]$_4$[Bi$_6$Mo$_3$(CO)$_9$] are presented in **Figures S17**. A deviation of the amount of K is rather common in the EDX characterization of Zintl clusters which can be attributed to the irregular surfaces of the crystals after exposing in air.
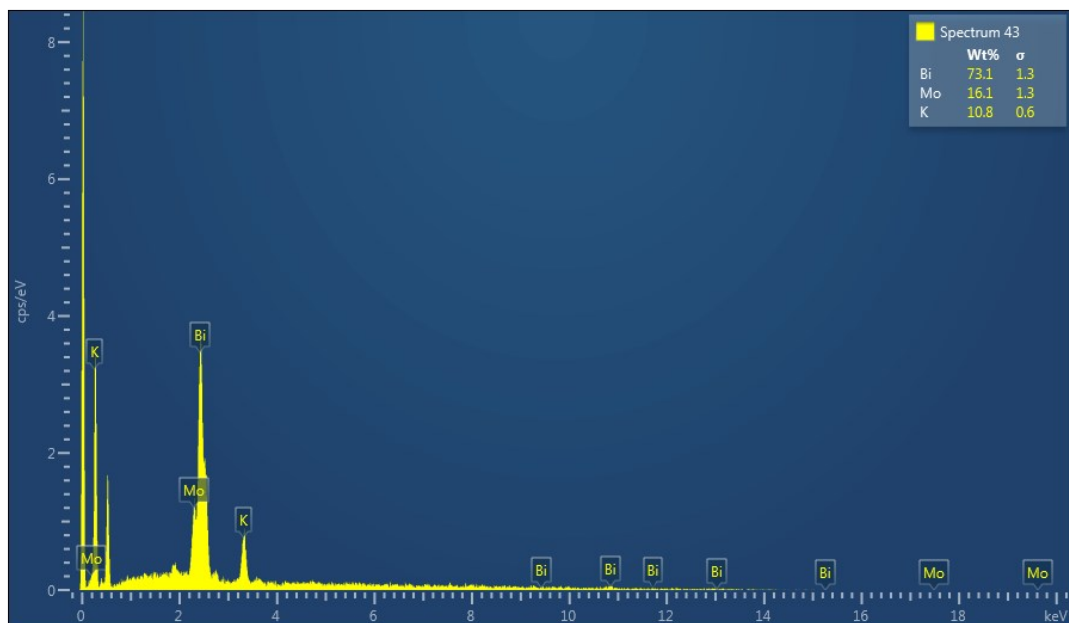
| Element | Line type | wt% | σ | Experimental / Calculated Atom % |
|---------|-----------|------|-----|----------------------------------|
| K | K series | 10.8 | 0.4 | 34.79/30.76 |
| Mo | L series | 16.1 | 0.9 | 21.14/23.07 |
| Bi | L series | 73.1 | 0.9 | 44.07/46.15 |

**Figure S17.** EDX analysis of $[K(2.2.2\text{-crypt})]_4[Bi_6Mo_3(CO)_9]$.

## 5. Cartesian Coordinates of Clusters Described in the Text.

$$[Bi_6Mo_3(CO)_9]^{4-}$$
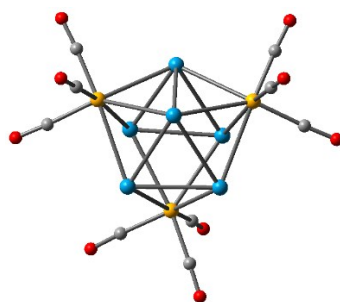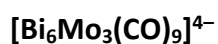


| | | | |
|----|-------------|-------------|--------------|
| Bi | 8.10370000 | 3.16170000 | 7.46820000 |
| Bi | 8.51800000 | 5.40600000 | 5.34600000 |
| Bi | 5.22270000 | 5.05030000 | 8.55250000 |
| Bi | 9.79710000 | 5.63290000 | 8.25460000 |
| Mo | 5.77990000 | 4.08440000 | 5.66160000 |
| Mo | 7.75720000 | 4.49540000 | 10.22510000 |

| Bi  | 5.96680000  | 7.06640000  | 6.29900000  |
|-----|-------------|-------------|-------------|
| Mo  | 8.81350000  | 8.14420000  | 6.73470000  |
| Bi  | 7.18510000  | 7.33320000  | 9.24050000  |
| C   | 4.83140000  | 2.48450000  | 6.21670000  |
| C   | 4.19490000  | 4.64300000  | 4.69680000  |
| C   | 6.29980000  | 3.16820000  | 4.03480000  |
| C   | 9.36880000  | 3.88430000  | 11.11100000 |
| C   | 6.89480000  | 2.83630000  | 10.74250000 |
| C   | 7.23400000  | 5.26420000  | 11.92610000 |
| C   | 9.84950000  | 9.24360000  | 7.94810000  |
| C   | 10.22860000 | 8.33020000  | 5.42650000  |
| C   | 8.02460000  | 9.75320000  | 6.00240000  |
| O   | 4.22760000  | 1.50690000  | 6.48510000  |
| O   | 10.31410000 | 3.48160000  | 11.69850000 |
| O   | 6.55250000  | 2.58170000  | 3.03800000  |
| O   | 6.92730000  | 5.67230000  | 12.99400000 |
| O   | 3.22100000  | 4.91300000  | 4.07890000  |
| O   | 6.40380000  | 1.83210000  | 11.12110000 |
| O   | 10.49870000 | 9.94800000  | 8.64120000  |
| O   | 7.60190000  | 10.76440000 | 5.55150000  |
| O   | 11.09990000 | 8.49850000  | 4.64270000  |

$$[\text{Ge}_9]^{2-}$$
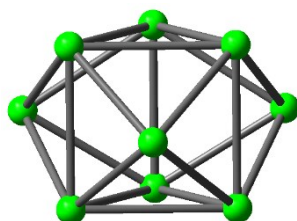


| Ge | -1.37975903 | 0.79660425  | 1.36627600  |
|----|-------------|-------------|-------------|
| Ge | -1.37975903 | 0.79660425  | -1.36627600 |
| Ge | -2.17514246 | -1.25581908 | -0.00000000 |
| Ge | 1.37975903  | 0.79660425  | 1.36627600  |
| Ge | 0.00000000  | 2.51163817  | -0.00000000 |
| Ge | -0.00000000 | -1.59320849 | -1.36627600 |
| Ge | 0.00000000  | -1.59320849 | 1.36627600  |
| Ge | 1.37975903  | 0.79660425  | -1.36627600 |
| Ge | 2.17514246  | -1.25581908 | -0.00000000 |

$$[\text{Ge}_9]^{4-}$$
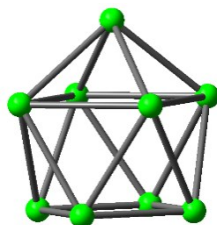
| Ge | 0.00000000  | 2.01659669  | 0.76355389  |
| Ge | -1.20367683 | -1.20367683 | -1.44915411 |
| Ge | 2.01659669  | 0.00000000  | 0.76355389  |
| Ge | 0.00000000  | -2.01659669 | 0.76355389  |
| Ge | 0.00000000  | 0.00000000  | 2.38271489  |
| Ge | -2.01659669 | -0.00000000 | 0.76355389  |
| Ge | 1.20367683  | 1.20367683  | -1.44915411 |
| Ge | 1.20367683  | -1.20367683 | -1.44915411 |
| Ge | -1.20367683 | 1.20367683  | -1.44915411 |

## 6. The Result of the AdNDP Analysis for Mo(CO)$_3$ Fragments in Cluster 1a.



(a) Nine s-type lone pairs on O atoms
ON=1.97 lel

(b) Nine 2c-2e C-O σ bonds
ON=2.00 lel

(c) Nine 2c-2e C-O π bonds
ON=2.00 lel

(d) Nine 2c-2e C-O π bonds
ON=2.00 lel

(e) Nine 2c-2e Mo-C σ bonds
ON=1.94-1.99 lel

(f) Three 3c-2e Mo-C-C σ bonds
ON=1.86-1.1.87 lel

(g) Three 3c-2e Mo-C-C σ bonds
ON=1.83-1.85 lel

h) Three 3c-2e Mo-C-C σ bonds
ON=1.82-1.83lel
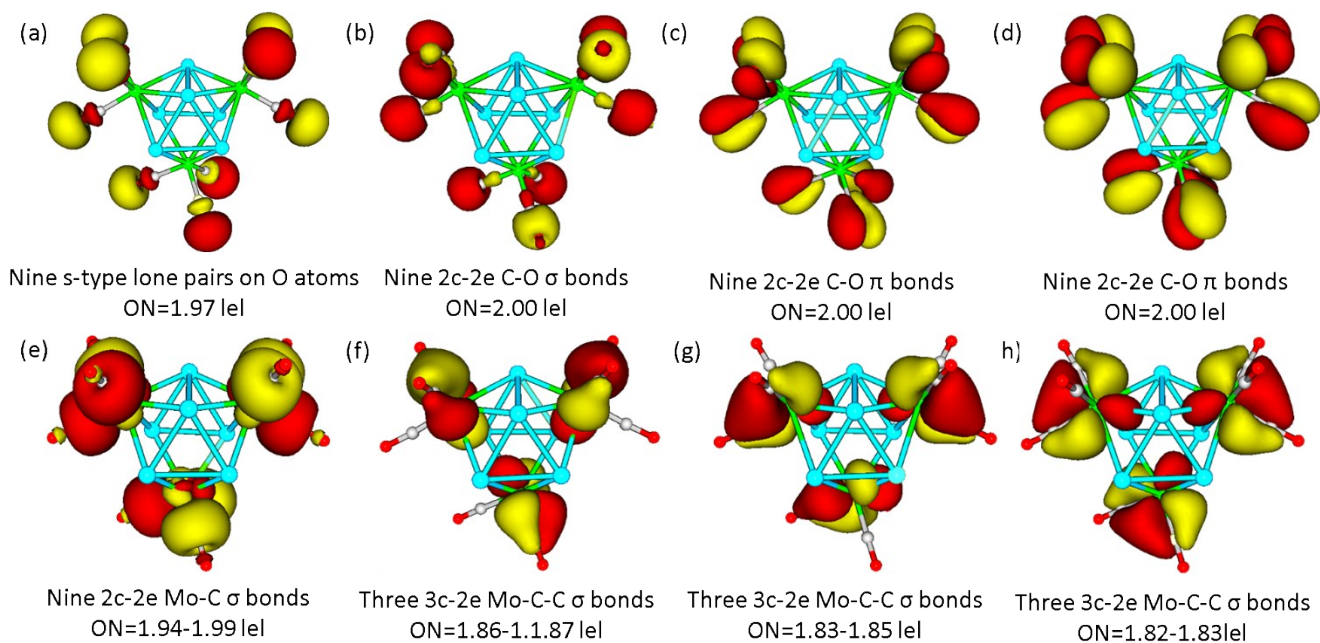
**Figure S18.** The AdNDP analysis for Mo(CO)$_3$ fragments in cluster [Bi$_6$Mo$_3$(CO)$_9$]$^{4-}$.

(a) Six s-lone pairs on Bi
ON=1.94-1.93 |e|

(b) Two 3c-2e σ bonds
ON=1.97 |e|

(c) Three 5c-2e σ bonds
ON=1.92-1.76 |e|

(d) Three 5c-2e σ bonds
ON=1.91-1.70 |e|

(e) Three 5c-2e σ bonds
ON=1.85-1.72 |e|

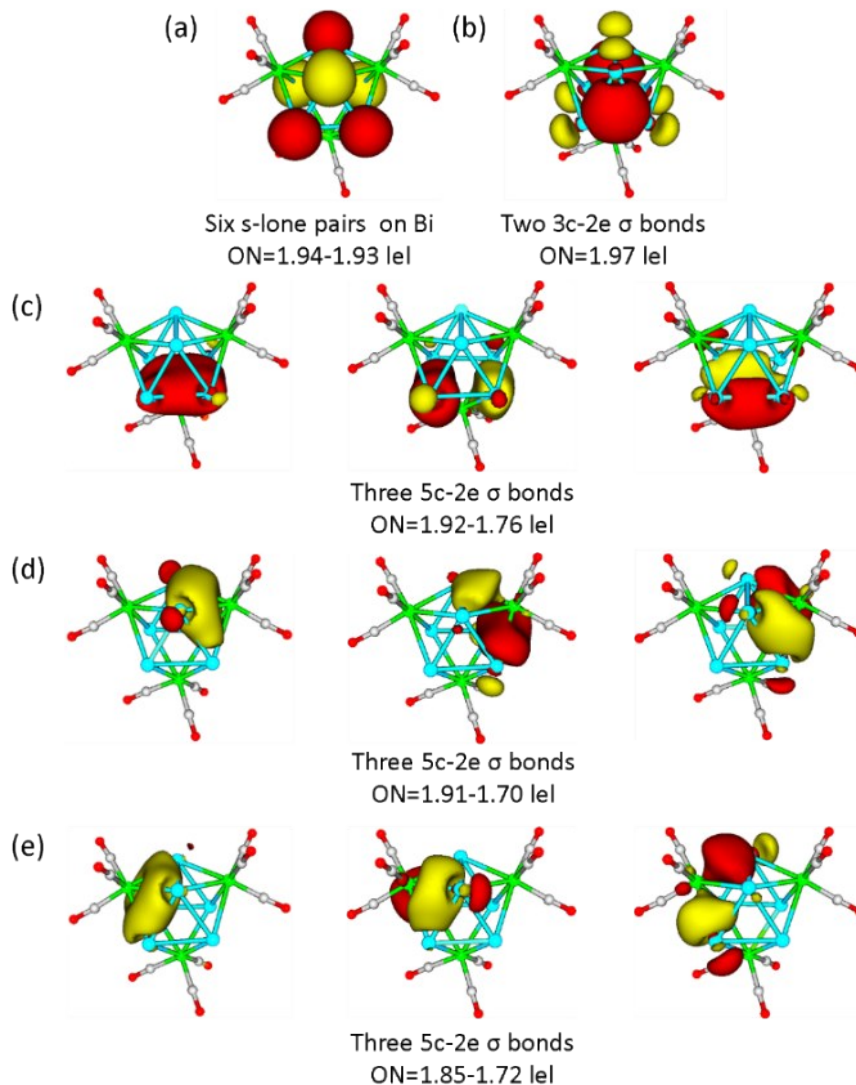**Figure S19.** The AdNDP analysis for the nine-atom cage in cluster $[Bi_6Mo_3(CO)_9]^{4-}$.

# References

(1) D. P. Tate, W. R. Knipple and J. M. Augl, *Inorg. Chem.*, 1962, **1**, 433-434.

(2) G. M. Sheldrick, *Acta Crystallogr. Sect. A: Found. Adv.*, 2015, **71**, 3-8.

(3) O. V. Dolomanov, L. J. Bourhis, R. J. Gildea, J. A. K. Howard and H. Puschmann, *J. Appl. Crystallogr.*, 2009, **42**, 339-341.

(4) A. L. Spek, *Acta Crystallogr., Sect. D: Biol. Crystallogr.*, 2009, **65**, 148-155.

(5) ADF2019.103; SCM: Amsterdam, 2019; http://www.scm.com.

(6) C. Adamo and V. Barone, *J. Chem. Phys.*, 1999, **110**, 6158-6170.

(7) D. Y. Zubarev and A. I. Boldyrev, *Phys. Chem. Chem. Phys.*, 2008, **10**, 5207-5217.

(8) M. J. Frisch, G. W. Trucks, H. B. Schlegel, G. E. Scuseria, M. A. Robb, J. R. Cheeseman, G. Scalmani, V. Barone, B. Mennucci, G. A. Petersson, H. Nakatsuji, M. Caricato, X. Li, H. P. Hratchian, A. F. Izmaylov, J. Bloino, G. Zheng, J. L. Sonnenberg, M. Hada, M. Ehara, K. Toyota, R. Fukuda, J. Hasegawa, M. Ishida, T. Nakajima, Y. Honda, O. Kitao, H. Nakai, T. Vreven, J. J. A. Montgomery, J. E. Peralta, F. Ogliaro, M. Bearpark, J. J. Heyd, E. Brothers, K. N. Kudin, V. N. Staroverov, T. Keith, R. Kobayashi, J. Normand, K. Raghavachari, A. Rendell, J. C. Burant, S. S. Iyengar, J. Tomasi, M. Cossi, N. Rega, J. M. Millam, M. J. Klene, E. Knox, J. B. Cross, V. Bakken, C. Adamo, J. Jaramillo, R. Gomperts, R. E. Stratmann, O. Yazyev, A. J. Austin, R. Cammi, C. Pomelli, J. W. Ochterski, R. L. Martin, K. Morokuma, V. G. Zakrzewski, G. A. Voth, P. Salvador, J. J. Dannenberg, S. Dapprich, A. D. Daniels, O. Farkas, J. B. Foresman, J. V. Ortiz, J. Cioslowski and D. J. Fox, GAUSSIAN 09 (Revision D.01), Gaussian, Inc., Wallingford CT, 2013.

(9) T. Lu and F. Chen, *J. Comput. Chem.*, 2012, **33**, 580-592.

(10) M. J. Frisch, G. W. Trucks, H. B. Schlegel, G. E. Scuseria, M. A. Robb, J. R. Cheeseman, G. Scalmani, V. Barone, G. A. Petersson, H. Nakatsuji, X. Li, M. Caricato, A. V. Marenich, J. Bloino, B. G. Janesko, R. Gomperts, B. Mennucci, H. P. Hratchian, J. V. Ortiz, A. F. Izmaylov, J. L. Sonnenberg, D. Williams-Young, F. Ding, F. Lipparini, F. Egidi, J. Goings, B. Peng, A. Petrone, T. Henderson, D. Ranasinghe, V. G. Zakrzewski, J. Gao, N. Rega, G. Zheng, W. Liang, M. Hada, M. Ehara, K. Toyota, R. Fukuda, J. Hasegawa, M. Ishida, T. Nakajima, Y. Honda, O. Kitao, H. Nakai, T. Vreven, K. Throssell, J. A. Montgomery, Jr., J. E. Peralta, F. Ogliaro, M. J. Bearpark, J. J. Heyd, E. N. Brothers, K. N. Kudin, V. N. Staroverov, T. A. Keith, R. Kobayashi, J. Normand, K. Raghavachari, A. P. Rendell, J. C. Burant, S. S. Iyengar, J. Tomasi, M. Cossi, J. M. Millam, M. Klene, C. Adamo, R. Cammi, J. W. Ochterski, R. L. Martin, K. Morokuma, O. Farkas, J. B. Foresman, and D. J. Fox, GAUSSIAN 16, Gaussian, Inc., Wallingford CT, 2016.

(11) E. van Lenthe, E.-J. Baerends and J. G. Snijders, *J. Chem. Phys.*, 1994, **101**, 9783–9792.

(12) Y. Zhang, A. Wu, X. Xu and Y. Yan, *Chem. Phys. Lett.*, 2006, **421**, 383–388.